Journal of Catalysis 263 (2009) 67–74

Contents lists available at ScienceDirect

Journal of Catalysis

www.elsevier.com/locate/jcat

# Effects of diffusion and particle size in a kinetic model of catalyzed reactions

T.G. Mattos [a], Fábio D.A. Aarão Reis [a,b,*]

[a] Instituto de Física, Universidade Federal Fluminense, Av. Litoranea s/n, Campus da Praia Vermelha, Niteroi RJ 24210 - 340, Brazil
[b] Department of Chemistry, University of Wisconsin, Madison, WI 53706, USA

ARTICLE INFO

*Article history:*
Received 1 December 2008
Revised 21 January 2009
Accepted 24 January 2009
Available online 10 February 2009

*Keywords:*
Catalysis
Diffusion
Desorption
Spillover
Back spillover
Scaling

ABSTRACT

We study a model for unimolecular reaction on a supported catalyst including reactant diffusion and desorption, using analytical methods and scaling concepts. For rapid reactions, enhancing surface diffusion or increasing particle size favors the flux of reactants to the catalyst particles, which increases the turnover frequency (TOF). The reactant flux towards the support becomes dominant when the ratio of diffusion lengths in the catalyst and in the support exceeds a critical value. A peak in the TOF is obtained for temperature-dependent rates if desorption energy in the support ($E_d$) exceeds those of diffusion ($E_D$) and reaction ($E_r$). Significant dependence on particle size is observed when the gaps between those energies are small, with small particles giving higher TOF. Slow reactions ($E_r > E_d$) give TOF monotonically increasing with temperature, with higher reactant losses in small particles. The scaling concepts can be extended to interpret experimental data and results of more complex models.



## 1. Introduction

Modeling heterogeneous catalytic processes is an essential tool for catalyst design and for the improvement of operating conditions [1–4]. Hierarchical approaches have to be adopted due to the need of information on a wide range of length and time scales, from the electronic structure to the reactor design [1]. An important step of this approach is the microkinetic modeling, where microscopic processes such as reaction, diffusion, aggregation, and desorption are described by stochastic rules, providing information on the efficiency of the catalytic process in length scales ranging from a few nanometers to several micrometers.

An important problem to be addressed with these methods is the effect of diffusion of reactants through the interface between the catalyst particle and the support. Several recent experimental papers illustrate these phenomena in catalyzed reactions [5–13] as well as in related problems, such as gas adsorption [14–16], where the same materials may be used. Morphological features of the catalyst and support and physico-chemical conditions of operation determine the role of diffusion on the performance of the process [2,17]. Sometimes these phenomena are called capture-zone effects, since a certain region of the support surrounding the particle may increase the effective area for capturing reactants from the gas phase, but there are also cases where a net flux to the support is observed. When only one phase can adsorb the reactant from the gas, the terms spillover (reactant flux from the catalyst to the support) or back spillover (the opposite flow) are used [18,19], although recently many authors have extended these terms to reactants adsorbing in both phases [2] (and here we will use them to facilitate the discussion of the results).

Due to the large interest in industry, some models which incorporated the effects of reactant diffusion through the catalyst-support interface were designed for certain applications. The simplest models are based on rate equations (mean-field models) that do not account for the spatial heterogeneity of the media where reactions take place [20–23], or that use some type of approximation to represent that heterogeneity [24,25]. Other models represent it through distributions of catalytic sites in lattices. Most of them are designed to describe CO oxidation in different catalysts and conditions [26–29], and simplify diffusion and adsorption processes of some species (although other applications have also been proposed [16,27,30,31]). In order to get a deeper insight on the effects of reactant diffusion, Cwiklik et al. [32,33] recently simulated simple reaction–diffusion models in surfaces with catalytic stripes and squares, as well as random distributions of catalytic sites. In certain ranges of parameters, they showed monotonic dependences of the turnover frequency (TOF) on diffusion coefficients and reaction rates [32].

A number of other papers aim at a full investigation of simple models of reaction and diffusion. In the present context, relevant examples are models in lattices with distributions of catalytic sites, i.e. with some type of non-homogeneity of catalytic activ-

* Corresponding author at: Instituto de Física, Universidade Federal Fluminense, Av. Litoranea s/n, Campus da Praia Vermelha, Niteroi RJ 24210 - 340, Brazil. Fax: +55 21 26295887.
*E-mail addresses:* tgmattos@if.uff.br (T.G. Mattos), reis@if.uff.br (F.D.A. Aarão Reis).

0021-9517/$ – see front matter 
doi:10.1016/j.jcat.2009.01.011

ity [34–39]. Even adsorption–desorption models without surface diffusion show that the correlations in catalyst particle position have nontrivial effects on the TOF, independently of adsorbate interactions [36,40,41]. Moreover, models including diffusion in heterogeneous surfaces show that the structures that maximize the efficiency of a catalytic process are highly dependent on the rates of the main microscopic processes [39].

In the present paper, we will propose a one-dimensional lattice model for unimolecular reactions in a supported catalyst, with reactant diffusion and desorption both in the support and in the catalyst particles. Our aim is to understand the interplay between these physico-chemical mechanisms, particle size and catalyst coverage. The model geometry is equivalent to that of Ref. [32], but here we will obtain an analytic solution that facilitates the illustration of different possible outcomes. We will use scaling concepts to explain the model results, so that this framework can be extended to more complex models and applications to real systems. Indeed, scaling approaches were already shown to be very useful to understand qualitative trends in reaction–diffusion models [42,43].

Among our results, we will distinguish conditions to enhance the net reactant flux from the catalyst to the support or vice-versa by varying one of the microscopic rates, and we will discuss the effect of increasing the catalyst particle size. The increase or decrease of the TOF will be shown to depend on the relation between diffusion lengths of reactants in the catalyst and in the support. Some of these results reinforce findings of previous works [27,28,32]. Moreover, under reasonable assumptions for temperature-dependent rates, we will show that a remarkable increase in the TOF can be obtained if reverse spillover regularly fills the catalytic particles with the reactants adsorbed in the support. This feature may be observed in a large temperature range, a possibility which is interesting for applications. The identification of these scenarios is possible because the model accounts for the inhomogeneity of the catalytic system and, consequently, predicts inhomogeneous distributions of reactants, which advances over the mean-field models.

## 2. The model

The physico-chemical processes involved in the model are illustrated in Fig. 1.

The catalyst particles are represented by segments of $l$ sites in a line, separated by $d$ support sites. Assuming that $a$ is the size of the lattice site, this corresponds to particles of diameter $la$ separated by a distance $da$. The fraction of the support covered by the catalytic material is

$$\epsilon \equiv \frac{l}{l+d}. \tag{1}$$

This lattice structure may be a reasonable description of some model catalysts [19,44], as well as a good approximation to the morphology of catalytic clusters supported in materials with long and narrow pores [45].

The particle size is determined by the physico-chemical conditions in which the catalytic material is deposited on the support [46]. The fraction of the support covered, $\epsilon$, is related to the amount of material used to produce a sample as well as the particle shape, which determines the surface to volume ratio. In oxide supported Pt or Pd catalysts, the particle diameter usually vary from 1 to 50 nm—depending on the growth conditions and if sintering occurs, sizes of 100 nm or more can be found. Since $a$ is of order of a few angstroms, this typically corresponds to $l$ ranging from 3 to 150 lattice sites. The spacing between the particles has a broad distribution in catalysts supported in porous materials, but in model catalysts they are nearly uniform, usually in the range 50–200 nm ($d$ typically between 100 and 500 lattice spacings for most oxide supports).

The flux of a single chemical species (reactant) towards the surface occurs with rate $F$, which is defined as the number of incoming molecules per site per unit time. In most of this work, $F$ will be used to define the time scale of the model, so that other frequencies are calculated relatively to this quantity. The reactant adsorbs in the (randomly chosen) site of incidence if it is empty, either in the catalyst or in the support, otherwise the adsorption attempt is rejected. Sticking coefficients are set equal to 1, since the effects of different values in the catalyst and in the support can be incorporated in the corresponding desorption rates: $k_d^s$ and $k_d^c$, in the support and in the catalyst particles, respectively (each rate corresponds to number of events per site per unit time). Interaction between the adsorbates is restricted to the excluded volume condition.

Adsorbed reactants diffuse with coefficient $D$, which for simplicity is assumed to be the same in the support and in the catalyst. It means that each reactant attempts to execute $2D/a^2$ random steps to nearest neighbor sites per unit time. We are assuming that the activation energy for diffusion is the same in those regions, which is certainly not true for a real catalyst. However, it is not a very restrictive assumption for our study because the results are interpreted in terms of diffusion lengths and scaling ideas are emphasized, allowing a direct extension to cases of different $D$ in different regions.

Since reactants are always in contact with the support or the catalyst, this is a surface diffusion model, which is a reasonable assumption on metal particles. On the other hand, Knudsen diffusion may be more realistic for the movement of reactants inside a catalyst pore. However, this does not represent a limitation because a suitable value of $D$ can be chosen, and interpretations based on diffusion lengths are still valid.

The adopted reaction mechanism for reactant A and product B is

$$A_{ads} \rightarrow B_{gas}, \tag{2}$$

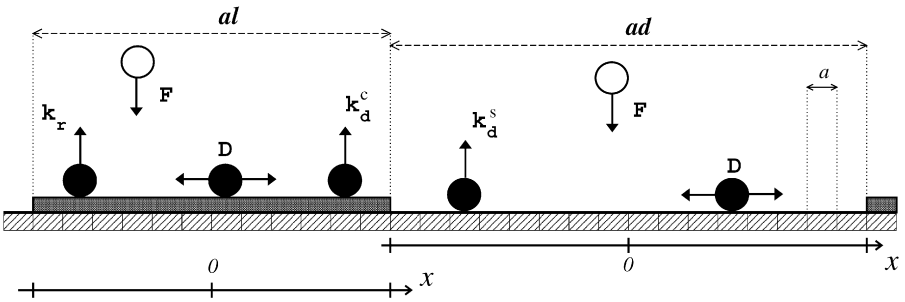


**Fig. 1.** Schematic representation of the model for the supported catalyst, with the rates of the physico-chemical processes. Non-adsorbed reactant A (Eq. (3)) is represented by white circles, while adsorbed reactant A is represented by black circles. The $x$ axis used in the analytic solution are shown (for the particle and for the support).

with reaction rate $k_r$ assumed to be uniform in the catalytic region (this rate corresponds to number of events per site per unit time). The unimolecular reaction (2) may represent an Eley–Rideal (ER) mechanism, in which the adsorbed species reacts with another species C arriving from the gas phase and forms a volatile product:

$$A_{ads} + C_{gas} \rightarrow B_{gas}. \tag{3}$$

For instance, an application to CO oxidation is discussed in Refs. [21,22]. In this case, $k_r$ not only accounts for activation of the adsorbed reactant but also for the flux of the other reactant from the gas phase. Certainly the assumption that $k_r$ is constant in the whole catalytic region is not realistic because it is well known that different crystalline faces of a metal have distinct catalytic activity. However, the present assumption is useful for a study which aims at investigating the interplay of many other different physicochemical processes.

## 3. Analytic solution

In order to solve the model analytically, we assume that the catalyst particles and the support segments between them are sufficiently large ($l \gg 1$, $d \gg 1$), so that a continuous approximation is possible. Although $l$ and $d$ may not be very large in real systems, we will show that the continuous approximation works well even with $l$ and $d$ of order 10.

The dimensionless reactant coverages in the catalyst particle and in the support are respectively defined as $\theta_c(x,t)$ and $\theta_s(x,t)$. For simplicity, we use the same variable $x$ for position in both regions, with the range $-la/2 \leqslant x \leqslant la/2$ in the catalyst and the range $-da/2 \leqslant x \leqslant da/2$ in the support. Diffusion, reaction and adsorption–desorption processes of Fig. 1 lead to equations for surface coverages; in the catalyst, we have

$$\frac{\partial}{\partial t}\theta_c(x,t) = D\frac{\partial^2}{\partial x^2}\theta_c(x,t) + F\big[1-\theta_c(x,t)\big] - \big(k_r + k_d^c\big)\theta_c(x,t), \tag{4}$$

and in the support we have

$$\frac{\partial}{\partial t}\theta_s(x,t) = D\frac{\partial^2}{\partial x^2}\theta_s(x,t) + F\big[1-\theta_s(x,t)\big] - k_d^s\theta_s(x,t). \tag{5}$$

Each of these equations is valid in the above defined ranges of $x$.

Here we are interested in steady state solutions, where

$$\frac{\partial}{\partial t}\theta_c(x,t) = \frac{\partial}{\partial t}\theta_s(x,t) = 0$$

and, consequently, $\theta_c$ and $\theta_s$ depend only on $x$. In the catalyst, this gives

$$D\frac{d^2\theta_c}{dx^2} + F(1-\theta_c) - \big(k_r + k_d^c\big)\theta_c = 0. \tag{6}$$

In the support, an analogous equation (without the reaction term) is obtained. Equation (6) can be easily solved and gives

$$\theta_c(x) = r_c + \alpha_c \cosh(x/\lambda_c), \tag{7}$$

where $\alpha_c$ is a constant to be determined from boundary conditions and

$$r_c \equiv \frac{1}{1 + k_r/F + k_d^c/F}, \qquad \lambda_c \equiv \sqrt{\frac{D/F}{1 + k_r/F + k_d^c/F}}. \tag{8}$$

Analogously, in the support we obtain

$$\theta_s(x) = r_s + \alpha_s \cosh(x/\lambda_s), \tag{9}$$

where $\alpha_s$ is a constant and

$$r_s \equiv \frac{1}{1 + k_d^s/F}, \qquad \lambda_s \equiv \sqrt{\frac{D/F}{1 + k_d^s/F}}. \tag{10}$$

Note that, as expected, diffusion, reaction and desorption rates appear in our results in the form of ratios to the external particle flux $F$.

The calculation of unknown constants in equations such as (7) and (9) usually follows from the use of suitable boundary conditions. However, here diffusion leads to a net flux of reactants from the catalyst to the support or vice-versa, which depends on the competition of all other processes along both regions. Thus, those unknown constants will be determined by matching the gain and loss terms in each region due to all those processes, and the net flux at the interfaces will be obtained from them.

In the catalyst, the contribution to the loss rate due to diffusion involves the probability of finding a reactant in the edge site of that region and of finding the neighboring support site empty (due to the excluded volume condition). Other contributions come from reaction and desorption along the particle. Thus, the loss in the coverage of the catalytic region per unit time is

$$\begin{aligned}(\Delta\theta_c)_{loss} &= \frac{2D}{a^2}(1-\theta^*)\theta^\dagger + \frac{1}{a}\int_{-la/2}^{la/2}\big(k_r + k_d^c\big)\theta_c(x')\,dx' \\ &= \frac{2D}{a^2}(1-\theta^*)\theta^\dagger + l\big(k_r + k_d^c\big)\bar{\theta}_c,\end{aligned} \tag{11}$$

where $\theta^*$ is the coverage of the edge site of the support region (neighbor of the catalyst)

$$\theta^* \equiv \theta_s\left(x = \frac{da}{2}\right) = r_s + \alpha_s \cosh\left(\frac{da}{2\lambda_s}\right), \tag{12}$$

$\theta^\dagger$ is the coverage of the edge site of the catalytic region (neighbor of the support)

$$\theta^\dagger \equiv \theta_c\left(x = \frac{la}{2}\right) = r_c + \alpha_c \cosh\left(\frac{la}{2\lambda_c}\right), \tag{13}$$

and $\bar{\theta}_c$ is the average coverage of the catalytic region

$$\bar{\theta}_c \equiv \frac{1}{la}\int_{-la/2}^{la/2}\theta_c(x')\,dx'. \tag{14}$$

The gain rate, which accounts for flux from the support to the catalyst at the edge sites and for the external flux, is

$$\begin{aligned}(\Delta\theta_c)_{gain} &= \frac{2D}{a^2}\theta^*\big(1-\theta^\dagger\big) + \frac{1}{a}\int_{-la/2}^{la/2}F\big[1-\theta_c(x')\big]\,dx' \\ &= \frac{2D}{a^2}\theta^*\big(1-\theta^\dagger\big) + lF(1-\bar{\theta}_c).\end{aligned} \tag{15}$$

Analogously, loss and gain terms can be determined for the support region, so that solutions for $\alpha_c$ and $\alpha_s$ are

$$\alpha_c = \frac{\lambda_c(r_s - r_c)\tanh\left(\frac{da}{2\lambda_s}\right)}{\lambda_c\cosh\left(\frac{la}{2\lambda_c}\right)\tanh\left(\frac{da}{2\lambda_s}\right) + \left[\lambda_s + a\tanh\left(\frac{da}{2\lambda_s}\right)\right]\sinh\left(\frac{la}{2\lambda_c}\right)}, \tag{16}$$

and

$$\alpha_s = \frac{\lambda_s(r_c - r_s)\tanh\left(\frac{la}{2\lambda_c}\right)}{\lambda_s\cosh\left(\frac{da}{2\lambda_s}\right)\tanh\left(\frac{la}{2\lambda_c}\right) + \left[\lambda_c + a\tanh\left(\frac{la}{2\lambda_c}\right)\right]\sinh\left(\frac{da}{2\lambda_s}\right)}. \tag{17}$$

The turnover frequency, which is the number of reactions per unit site and unit time, is given by

$$TOF = k_r\bar{\theta}_c. \tag{18}$$

We simulated the discrete model, as defined in Section 2 (see also Fig. 1), in order to check the accuracy of the analytic solution when

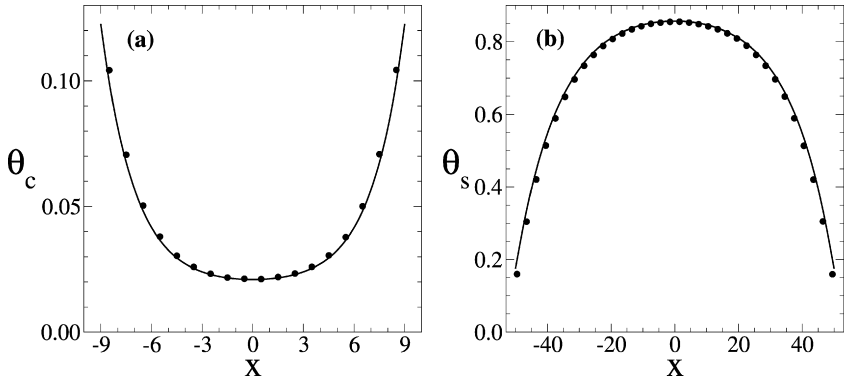


**Fig. 2.** Reactant coverage as a function of the position $x$ along (a) the catalyst and (b) the support, for $2D/(a^2F) = 420$, $k_d^s/F = 0.1$, $k_r/F = 8$, $d = 100$ and $l = 18$. Circles are simulation results and the curves are analytical results.

$l$ and $d$ are not very large. Typical simulations consisted in 100 realizations of the process in a lattice with $L = 2^{17}$ sites and catalyst coverage near 15%. At each step, an attempt to deposit a new reactant at a randomly chosen site is done. Subsequently, the numbers of attempts to move reactants, desorb them and perform reactions are chosen proportional to the respective rates ($D$, $k_d^s$, $k_d^c$, $k_r$). Simulations begin with an empty lattice and proceed up to a long time after a steady state has been reached, where the coverages of both regions are constant.

We observe that even for $l \sim 10$ the continuous approximation is good. This is illustrated in Figs. 2a and 2b, where we compare the analytic and numerical results for the coverage distribution in the catalyst and in the support, respectively, using $l = 18$ and $d = 100$. Slight deviations are only found near the boundaries of those regions, but are always smaller than 5% for small $l$. The accuracy in the average coverages and in the TOF is usually higher.

Here the model was solved in the steady state, but it certainly can be extended to other situations, for instance when a finite amount of the reactant flows to the catalyst surface and the TOF changes in time. Other possibilities are the explicit incorporation of sticking probabilities and the assumption of different diffusion coefficients in the particles and in the support. The one-dimensional structure facilitates the solution, while preserving essential ingredients such as the spatial heterogeneity.

## 4. Results

In order to understand the role of the different rates from a scaling approach, we consider the diffusion lengths in the catalyst particle and in the support. If the corresponding region is large enough, the diffusion length measures the typical distance a reactant moves on it before reacting or desorbing. On the other hand, if the length of that region is smaller than the diffusion length, then it is expected that the reactant reaches its border and can flow to a neighboring domain.

In the catalyst, the average lifetime of an adsorbed species before reacting or desorbing is $\tau_c \sim 1/(k_r + k_d^c)$. During this time, it executes random walks with diffusion coefficient $D$, thus the average distance it spans is of order $(D\tau_c)^{1/2}$. This is the so-called diffusion length,

$$L_c = \sqrt{\frac{D}{k_r + k_d^c}}. \tag{19}$$

Analogously, a reactant in the support has a typical lifetime $1/k_d^s$, thus the corresponding diffusion length is

$$L_s = \sqrt{\frac{D}{k_d^s}}. \tag{20}$$

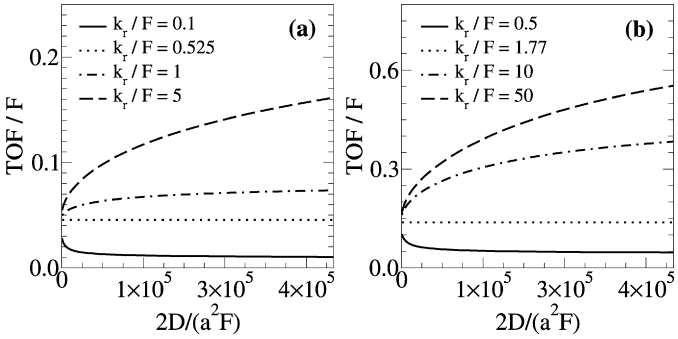


**Fig. 3.** Normalized turnover frequency as a function of diffusion coefficient for several reaction rates, with $k_d^c/F = 10^{-3}$, $k_d^s/F = 10$ and $l = 75$. Fractions of support covered are (a) $\epsilon = 0.05$ and (b) $\epsilon = 0.15$.

These expressions can be easily generalized to the case of different diffusion coefficients in the particles and in the support, which means that interpretations based on these quantities have a broader applicability.

We will consider cases where desorption in the catalytic region is very low, i.e. $k_d^c \ll F$, $k_d^s, k_r, 2D/a^2$. The values of all rates presented below are given relatively to the incident flux rate $F$, thus they are all dimensionless (setting $F = 1\ s^{-1}$ and the value of the parameter $a$, we would get the other ones in SI units). The TOF is also expressed relatively to $F$, thus it is limited to a maximum $\mathrm{TOF}/F = 1$.

In order to facilitate the presentation of the results, hereafter we will use the terms spillover and back spillover to denote a net flux of reactants by diffusion from the catalyst to the support and vice-versa, respectively. As noted above, the broader use of these terms follows a trend of some recent works [2,21–23,29,32].

### 4.1. Effects of reactant mobility and catalyst geometry

First we distinguish the conditions where either spillover or back spillover is dominant as the reactant mobility in the surface increases. In Figs. 3a and 3b we show the normalized TOF as a function of $2D/a^2$ for several reaction rates, respectively with fractions of support covered $\epsilon = 0.05$ and $\epsilon = 0.15$, and the same particle size $l = 75$.

Even without reactant diffusion ($D = 0$), the TOF significantly varies with $k_r$ because a large area of the catalyst may be poisoned for low reaction rates; for instance, in Fig. 3a we have normalized $\mathrm{TOF} = 0.0278$ and $0.0546$ for $k_r/F = 0.1$ and $k_r/F = 5$, respectively. Indeed, excluded volume effects limit the adsorption process, which is known to be a relevant effect even in mean-field models [3]. The increase of diffusion coefficient improves the catalytic process for high reaction rates, since back spillover effects

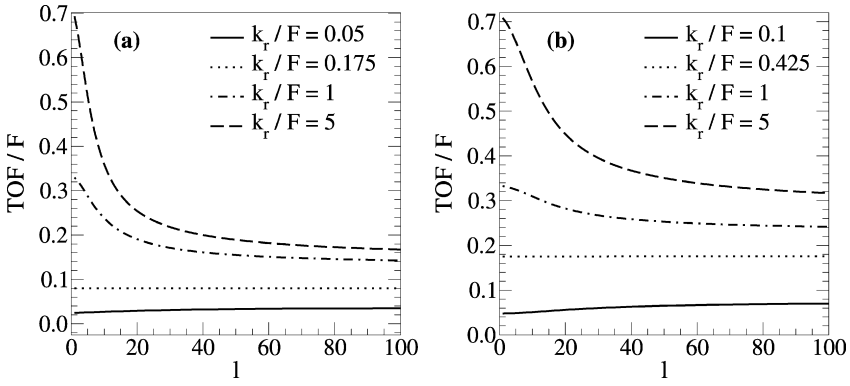


**Fig. 4.** Normalized turnover frequency as a function of catalyst particle size for several reaction rates, using $k_d^c/F = 10^{-3}$, $k_d^s/F = 1$ and $2D/(a^2F) = 500$. Fractions of support covered are (a) $\epsilon = 0.15$ and (b) $\epsilon = 0.3$.

are dominant as $D$ increases. However, with low reaction rates, the opposite effect is observed: reactants more easily leave the particles as $D$ increases, going to the support where they rapidly desorb. In Fig. 3a, there is no change in the normalized TOF as $D$ increases for $k_r/F = 0.525$, which corresponds to $L_s/L_c \approx 0.23$. If other values of the rates and other values of $l$ are chosen, the same feature is observed for a different value of $k_r$, but with the same ratio $L_s/L_c$. On the other hand, in Fig. 3b ($\epsilon = 0.15$), that feature is observed when $L_s/L_c \approx 0.42$. Thus, the critical ratio $L_s/L_c$ which separates regimes of rapid and slow reactions depends only on the fraction of support covered $\epsilon$; above (below) the critical ratio, back spillover (direct spillover) is dominant. This result can be interpreted as follows: if the relative increase of diffusion length in the support is larger (smaller) than that in the catalyst, then more reactants flow towards the particles (support) and the TOF increases (decreases).

Now we consider the effects of particle size. We consider changes in $l$ with fixed $\epsilon$, in order to simulate cases where a fixed amount of catalytic material is deposited on the support, but islands of different sizes are formed. Under these conditions, it is important to stress that the size of the gaps between particles ($d$) also increases when $l$ increases (Eq. (1)).

In Figs. 4a and 4b we show the normalized TOF as a function of the particle size $l$ for two different fractions of the support covered and various reaction rates. Again we observe regimes of high and low reaction rates, corresponding to high and low ratios $L_s/L_c$. For large reaction rates, decreasing $l$ is favorable, since $d$ also decreases ($\epsilon$ is fixed) and facilitates the back spillover. On the other hand, for low reaction rates, the conversion is improved by increasing the particle size, since the reactants spend longer times in larger catalytic regions, which compensates the increased desorption in the support. In other words, the loss due to decreasing back spillover is compensated by a gain in decreasing spillover. The same ratios $L_s/L_c$, which depend on the fraction of support covered $\epsilon$, separate the two regimes.

These nontrivial effects of the catalyst geometry may be helpful for catalyst design if one is interested in taking advantage of back spillover, preferrably in the case of rapid reactions, or in reducing the effect of spillover in the case of slow reactions. At this point, it is important to notice that Figs. 3 and 4 show that the change in one model parameter may increase the TOF by a factor near 3, which is a remarkable change in the efficiency of the catalytic process.

As far as we know, this is the first work that analyzes the conditions for changing the direction of the net reactant flux in the particle-support interface. The interpretation of results based on diffusion lengths was formerly proposed in Refs. [27,28] for models of CO oxidation in oxide supports. However, both studies focused on the regime where back spillover is dominant, for instance by assuming infinite diffusion lengths of some species adsorbed in the particles. That regime was also considered in Ref. [25] with a mean-field approach that accounts for the different neighborhood of the catalytic sites (in an approximate form). In this case, the approximation is successful because the diffusion lengths are small.

### 4.2. Temperature effects

The diffusion coefficient and the reaction and desorption rates are expected to have Arrhenius forms as follows:

$$D = \frac{a^2}{2}\nu_D \exp\left(-\frac{E_D}{k_B T}\right), \tag{21}$$

$$k_d^s = \nu_d \exp\left(-\frac{E_d}{k_B T}\right), \tag{22}$$

and

$$k_r = \nu_r \exp\left(-\frac{E_r}{k_B T}\right). \tag{23}$$

Here, $\nu_i$ is a frequency and $E_i$ is an activation energy ($i = D, d, r$). Assuming that the activation energy for desorption in the catalyst particles is much larger than the other activation energies, we use $k_d^c/F = 10^{-3}$, which is negligible compared to the other rates in the relevant temperature ranges. For the other activation energies, we always assume that $E_D < E_d$ [47].

Other reasonable assumptions on the amplitudes of the Arrhenius rates facilitate the analysis of the effects of different ranges of energy barriers. We will consider $\nu_D = \nu_r = 2 \times 10^{12}$ s$^{-1}$, $a = 5$ Å, and work with a range of ratios $\nu_d/\nu_r$ from 10 to 1000. These relations are reasonable for Langmuir–Hinshelwood (LH) reactions and for CO adsorption in oxides [2,28,47], respectively, but we emphasize that these systems are only rough guides to choose working parameters, and may not be viewed as prospective applications indeed, the unimolecular reaction of our model is representative of ER mechanism. In the following, we also consider fraction of support covered $\epsilon = 0.15$ and $F = 1$ s$^{-1}$ (thus the calculated rates are again ratios to $F$).

Qualitatively, we expect that each microscopic process will be significantly activated when its rate exceeds the external flux $F$. However, excluded volume effects lead to surface poisoning when reactions are not frequent (low temperatures), so that other processes can affect the turnover frequency only after reactions are activated.

#### 4.2.1. The cases $E_r > E_d$ and $E_r < E_D$

First we consider the simplest case where reactions are very difficult compared to the other activated processes, i.e. $E_r > E_d$. An example of slow reaction is the hydrogenation of CO on Pt [13],

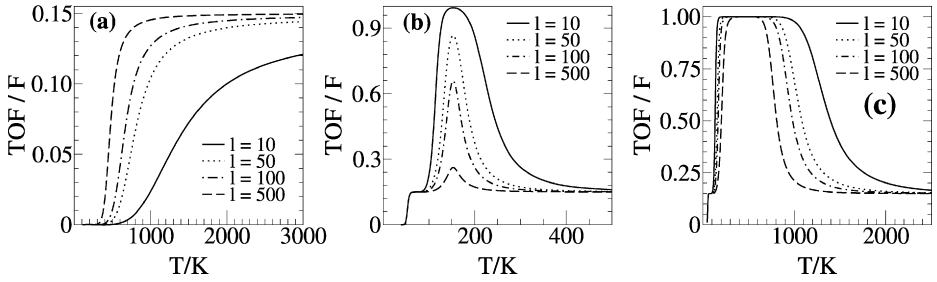


**Fig. 5.** Normalized turnover frequency as a function of temperature for several particle sizes, with: (a) $E_D = 5$ kcal/mol, $E_r = 15$ kcal/mol and $E_d = 10$ kcal/mol; (b) $E_D = 5$ kcal/mol, $E_r = 3$ kcal/mol and $E_d = 10$ kcal/mol; (c) $E_D = 6$ kcal/mol, $E_r = 3$ kcal/mol and $E_d = 35$ kcal/mol. In all cases, $\nu_d/\nu_r = 100$.

when compared to the spillover to the $TiO_2$ support and the formation of $CH_3O$ there.

Fig. 5a shows the typical evolution of the TOF with temperature for different particle sizes. When the reactions become more frequent ($k_r \sim F$, i.e. $T \sim 270$ K), desorption is already activated and diffusion is very fast. Thus spillover and subsequent desorption of reactants does not allow the increase of the turnover frequency. Instead, the TOF begins to increase only when $k_r \sim k_d$ ($T \sim 550$ K). At higher temperatures, the negative contribution of spillover is more important when the particles are small, so that a slow increase of the TOF is observed. On the other hand, this negative contribution is reduced for large particles, and the maximum TOF is rapidly attained by increasing the temperature. The value $\mathrm{TOF}/F \approx 0.15$ corresponds to the fraction of the surface covered by the catalyst, which is expected at high temperatures because only species adsorbed on the catalyst react.

Next we consider the case where reactions are easily excited, i.e. $E_r < E_D$. An example of rapid reaction with ER mechanism is CO oxidation on $Pd/CeO_2$ [21], where reaction rates are nearly 100 times larger than back spillover rates of oxygen.

Figs. 5b and 5c illustrate the case $E_r < E_D$ with small and large desorption energies, respectively.

In Fig. 5b, the TOF increases towards a plateau in $\mathrm{TOF}/F \approx 0.15$ at $T \sim 50$–$60$ K, where $k_r \sim F$. At $T \sim 100$ K, when diffusion is activated, back spillover leads to a second jump in the TOF, which is highly dependent on the particle size. For smaller sizes (small gaps between particles), the migration of reactants from the support to the catalyst is easy even for low $D$, thus large conversion rates are rapidly obtained. The temperature of maximal TOF is attained when desorption begins to play a significant role ($k_d^s \sim F$), independently of particle size. In the case of large gaps between the particles, this temperature is still low for back spillover to be efficient, thus only a small peak appears in the TOF plot. For further temperature increase, $l$-dependent results are again obtained. The diffusion length in the support is

$$L_s = \sqrt{\frac{\nu_D a^2}{\nu_d}}\exp\left[(E_d - E_D)/2k_BT\right],$$

which decreases with increasing temperature, and the beneficial effect of back spillover ceases when $L_s \sim l$; this condition is satistified at higher temperatures for smaller $l$, which explains the slower decay of the TOF in this case. For these reasons, the peak in the TOF is high and broad for small $l$, low and narrow for large $l$.

In Fig. 5c, the main features of Fig. 5b are present. However, since $E_d$ is much larger than the other activation energies, the maximal effect of back spillover ($\mathrm{TOF}/F \approx 1$) is observed in a wider temperature range and for all particle sizes shown there. Thus, Fig. 5b illustrates typical conditions in which particle size effects are clearer: desorption in the support has higher activation energy than diffusion and reactions, but activation of a process begins while the other processes are not fully activated, so that the diffusion length $L_s$ cannot attain large values before desorption is activated.

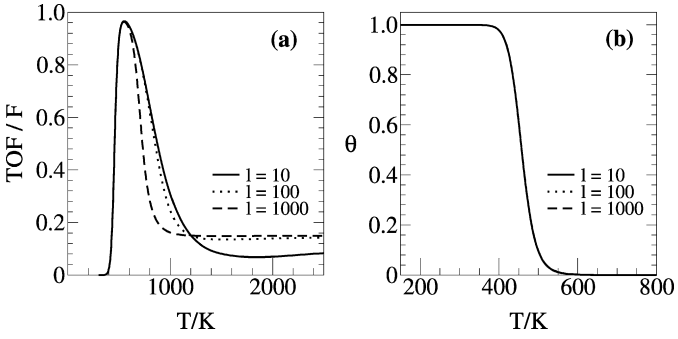


**Fig. 6.** (a) Normalized turnover frequency as a function of temperature for several particle sizes, with $E_D = 6$ kcal/mol, $E_r = 24$ kcal/mol, $E_d = 35$ kcal/mol, and $\nu_d/\nu_r = 100$. (b) Temperature dependence of the corresponding average reactant coverage.

*4.2.2. The case of intermediate reaction energies*

Now we consider cases of intermediate activation energies for reaction, i.e. $E_D < E_r < E_d$. CO oxidation provides several examples with such relation between activation energies; however, it is important to stress the difference in the usual reaction mechanism (LH instead of ER). An example is CO oxidation on $Pt/CeO_2$ [29]: the energy of diffusion of O on the support is 18 kcal/mol, while reaction energy is 27 kcal/mol and desorption in the support is 60 kcal/mol (diffusion on the catalyst is assumed to be fast for the application of a mean-field model in Ref. [29]).

In Fig. 6a we show the normalized TOF as a function of temperature for our model with three different particle sizes, using a set of activation energies previously suggested for CO oxidation in Pt(111) and $\nu_d = 100\nu_r$ [2]. Fig. 6b shows the evolution of the average coverage (particle plus support).

At low temperatures, all the surface is poisoned, and reactions are slow. Increasing the temperature to $T \sim 400$ K ($k_r \sim F$), the turnover frequency increases, thus vacancies are created in the particles and in the support, which facilitates the back spillover effects. Note that there is no significant effect of particle size when a large temperature range is scanned, since the diffusion lengths $L_s$ and $L_c$ are very large (diffusion is highly activated in much lower temperatures). While the TOF increases with temperature, the coverage rapidly decreases towards zero because diffusion and reaction are rapid compared to the external flux. Further temperature increase leads to a maximum in the turnover frequency, again when desorption in the support is activated ($k_d^s \sim F$). However, in the right side of the peaks of Fig. 6a, we observe a size dependence because back spillover ceases only when $L_s \sim l$. At high temperatures, a size dependence is also noticeable: small particles lose more reactants by spillover than the large ones, and those reactants easily desorb in the support, which leads to smaller TOF.

As explained above, the most remarkable effects of particle size are observed in cases where the activation energies are close to each other. This is also illustrated in Figs. 7a and 7b for $E_D < E_r < E_d$, but $E_D$ close to $E_r$, with different ratios between $\nu_r$ and $\nu_d$. In

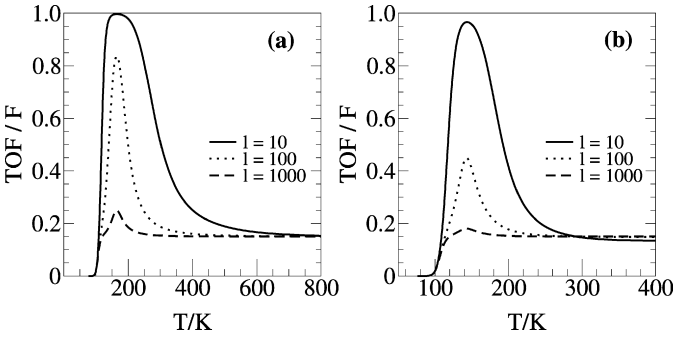


**Fig. 7.** Normalized turnover frequency as a function of temperature for several particle sizes, with $E_D = 5$ kcal/mol, $E_r = 6$ kcal/mol, $E_d = 10$ kcal/mol: (a) $\nu_d/\nu_r = 10$; (b) $\nu_d/\nu_r = 1000$.

this case, when reactions become more frequent and leave room for new incoming reactants ($k_r \sim F$), the surface mobility is still low (i.e. $2D/a^2$ is not much larger than $F$). Thus, back spillover is significant only for small particles (and small vacancies between them). However, if the spacing between particles is large, then slow diffusion is not able to bring all reactants adsorbed in the support to the catalytic region. Figs. 7a and 7b also show that these effects appear in a wider temperature range when the amplitudes of the Boltzmann factors are closer to each other, since activation of desorption occurs in higher temperatures.

## 5. Discussion

The aim of the present work is not the quantitative description of a particular catalytic process, but to discuss the interplay of various physico-chemical mechanisms and conditions in systems where spillover is present. However, it may be useful in the interpretation of some experimental results and motivate the proposal of extended models for their quantitative description.

Here we mention two recent works as examples where the scaling ideas developed above may be relevant. However, we emphasize the fact that our model cannot be directly applied to these systems, thus our results only suggest general guidelines to understand their qualitative behavior. In the first example, Piccolo and Henry [5] studied the oxidation of CO by NO on Pd/MgO and observed a peak in the TOF as a function of the temperature. They found a remarkable increase in the peak height as the particle size was decreased (even being accompanied by a decrease in the Pd coverage), but tiny shifts in the temperature of the maximum. These results resemble those in Figs. 6a, 7a and 7b. While the size-independent curve shape suggests weak size-dependence of activation energies, the peak height increase suggests that diffusion lengths of reactants were not very large when reactions were activated, so that back spillover (which increases TOF for any type of reaction) was facilitated with small particles. Thus, differences in activation energies of diffusion, reaction and desorption are probably small, with $E_d$ being larger than the other ones. The second example is a study of CO oxidation on Au on active supports (i.e. those which adsorb and supply oxygen to the reaction), which shows a different trend [48]: under certain conditions, the TOF does not depend on catalyst particle size. Although that reaction involves two species and is probably of LH type, the experimental result suggests that diffusion was highly activated at the working temperature. In this situation, similarly to our model, diffusion lengths are always very large and the contribution of back spillover does not depend on particle size.

Recalling the results of models for ethene and acetylene hydrogenation which incorporate spillover effects is also interesting at this point [30,31]. In both systems, the hydrocarbon blocks catalytic sites at high pressures, which leads to a discontinuity of the TOF when the external reactant flux towards a catalytic site is of the same order of the microscopic reaction rate. In ethene hydrogenation, this effect is shown to be more intense with small particles [30], leading to finite-size effects. However, diffusion is weakly activated at the working temperature when compared to the other processes (the amplitudes of Boltzmann factors associated to different processes are very different in that case), thus there is no significant effect of diffusion in the TOF. This reinforces the conclusion that the scaling approach proposed here can be extended to interpret more complex reaction models. This is very important in cases where analytic solutions are not feasible because it may help choosing the conditions to perform simulation work.

## 6. Conclusion

We proposed a model for a unimolecular reaction in a supported catalyst with tunable particle size and fraction of support covered. It represents important physico-chemical processes, such as diffusion, desorption and the external flux of reactants. We analyzed the effects of reactant exchange between particle and support on the turnover frequency under different conditions. The possibility of extending our scaling ideas and methods to experiments and to more complex models was also discussed. First we considered the isolated effects of enhancing surface diffusion (coefficient $D$) and increasing catalyst particle size $l$. For rapid reactions, the increase of any of those quantities favors back spillover and, consequently, increases the turnover frequency. This regime is separated from that dominated by spillover by a critical value of diffusion length in the catalyst and in the support, which depends only on the fraction of the support surface covered by the catalyst. In the spillover-dominated regime (slow reactions), increasing $D$ or $l$ slows down the conversion of the reactants. Subsequently, we considered temperature effects by assuming Arrhenius dependence of all physico-chemical rates and reasonable values for the amplitudes in those relations. With activation energy for desorption ($E_d$) in the support larger than that for diffusion ($E_D$), a peak in the turnover frequency as a function of temperature is observed for small and intermediate values of reaction activation energy $E_r$, i.e. for cases where $E_r < E_d$. Significant particle size dependence in the peaks is usually observed when the gaps between those energies are small, so that activation of one process occurs while the other ones are not fully activated yet, and the corresponding diffusion lengths rapidly vary with temperature. The right side of those peaks show size-dependence under more general conditions. For fixed amount of catalytic material deposited on the support, small particle sizes (with small distance between them) allow the turnover frequency to attain high peak values due to the beneficial effect of back spillover, while large particles provide low enhancements of catalytic activity. Finally, in the case of slow reactions ($E_r > E_d$), the TOF monotonically increases with temperature, and large particle sizes are more efficient to avoid the negative effects of direct spillover.

## Acknowledgments

The authors thank Prof. Robert Hamers for a critical reading of the manuscript and acknowledge support from CNPq and Faperj (Brazilian agencies) to their simulation laboratory at UFF, Brazil. TGM acknowledges a grant from CAPES (Brazil) and FDAAR acknowledges support from CNPq for his visit to UW–Madison.

## References

[1] L.J. Broadbelt, R.Q. Snurr, Appl. Catal. A Gen. 200 (2000) 23.
[2] V.P. Zhdanov, B. Kasemo, Surf. Sci. Rep. 39 (2000) 25.

[3] H. Lynggaard, A. Andreasen, C. Stegelmann, P. Stoltze, Prog. Surf. Sci. 77 (2004) 71.
[4] D.Y. Murzin, Ind. Eng. Chem. Res. 44 (2005) 1688.
[5] R. Piccolo, C.R. Henry, Appl. Surf. Sci. 162 (2000) 670.
[6] H. Chen, H. Yang, Y. Briker, C. Fairbridge, O. Omotoso, L. Ding, Y. Zheng, Z. Ring, Catal. Today 125 (2007) 256.
[7] K. Polychronopoulou, A.M. Efstathiou, Catal. Today 116 (2006) 341.
[8] A. Kecskeméti, T. Bánsági, F. Solymosi, Catal. Lett. 116 (2007) 101.
[9] M. Laurin, V. Johánek, A.W. Grant, B. Kasemo, J. Libuda, H.-J. Freund, J. Chem. Phys. 123 (2005) 054701.
[10] E. Odier, Y. Schuurman, C. Mirodatos, Catal. Today 127 (2007) 230.
[11] R. Marques, S. Capela, S. Da Costa, F. Delacroix, G. Djega-Mariadassou, P. Da Costa, Catal. Commun. 9 (2008) 1704.
[12] M. Bowker, E. Fourré, Appl. Surf. Sci. 254 (2008) 4225.
[13] T.F. Mao, J.L. Falconer, J. Catal. 123 (1990) 443.
[14] A.D. Lueking, R.T. Yang, Appl. Catal. A Gen. 265 (2004) 259.
[15] G. Dutta, U.V. Waghmare, T. Baidya, M.S. Hegde, Chem. Mater. 19 (2007) 6430.
[16] P. Jain, D.A. Fonseca, E. Schaible, A.D. Lueking, J. Phys. Chem. C 111 (2007) 1788.
[17] C.R. Henry, Surf. Sci. Rep. 31 (1998) 231.
[18] W.C. Conner, J.L. Falconer, Chem. Rev. 95 (1995) 759.
[19] J. Libuda, H.-J. Freund, Surf. Sci. Rep. 57 (2005) 157.
[20] J. Hoffmann, I. Meusel, J. Hartmann, J. Libuda, H.-J. Freund, J. Catal. 204 (2001) 378.
[21] C.N. Costa, S.Y. Christou, G. Georgiou, A.M. Efstathiou, J. Catal. 219 (2003) 259.
[22] S.Y. Christou, A.M. Efstathiou, Top. Catal. 42–43 (2007) 351.
[23] A. Galdikas, D. Duprez, C. Descorme, Appl. Surf. Sci. 236 (2004) 342.
[24] D.J. Dooling, J.E. Rekoske, L.J. Broadbelt, Langmuir 15 (1999) 5846.
[25] L. Cwiklik, Chem. Phys. Lett. 449 (2007) 304.
[26] C.R. Henry, C. Chapon, C. Duriez, J. Chem. Phys. 95 (1991) 700.
[27] A.S. McLeod, Catal. Today 53 (1999) 289.
[28] V.P. Zhdanov, B. Kasemo, J. Catal. 170 (1997) 377.
[29] S. Johansson, L. Österlund, B. Kasemo, J. Catal. 201 (2001) 275.
[30] A.S. McLeod, Chem. Eng. Res. Des. 82 (2004) 945.
[31] A.S. McLeod, R. Blackwell, Chem. Eng. Sci. 59 (2004) 4715.
[32] L. Cwiklik, B. Jagoda-Cwiklik, M. Frankowicz, Surf. Sci. 572 (2004) 318.
[33] L. Cwiklik, B. Jagoda-Cwiklik, M. Frankowicz, Appl. Surf. Sci. 252 (2005) 778.
[34] G. Oshanin, A. Blumen, J. Chem. Phys. 108 (1998) 1140.
[35] O. Bénichou, M. Coppey, M. Moreau, G. Oshanin, J. Chem. Phys. 123 (2005) 194506.
[36] G. Oshanin, M.N. Popescu, S. Dietrich, Phys. Rev. Lett. 93 (2004) 020602.
[37] E.V. Albano, J. Chem. Phys. 94 (1991) 1499.
[38] E.V. Albano, Phys. Rev. E 48 (1993) 913.
[39] A.P.J. Jansen, C.G.M. Hermse, Phys. Rev. Lett. 83 (1999) 3673.
[40] M. Rieger, J. Rogal, K. Reuter, Phys. Rev. Lett. 100 (2008) 016105.
[41] G. Oshanin, O. Bénichou, A. Blumen, J. Stat. Phys. 112 (2003) 541.
[42] F.D.A.A. Reis, J. Stafiej, J.-P. Badiali, J. Phys. Chem. B 110 (2006) 17554.
[43] F.D.A.A. Reis, J. Stafiej, Phys. Rev. E 76 (2007) 011512.
[44] G.A. Somorjai, R.L. York, D. Butcherab, J.Y. Parka, Phys. Chem. Chem. Phys. 9 (2007) 3500.
[45] F. Schüth, Annu. Rev. Mater. Res. 35 (2005) 209.
[46] H.-J. Freund, Surf. Sci. 500 (2002) 271.
[47] R. Gomer, Rep. Prog. Phys. 53 (1990) 917.
[48] M.M. Schubert, S. Hackenberg, A.C. van Veen, M. Muhler, V. Plzak, R.J. Behm, J. Catal. 197 (2001) 113.